

HIGH PERCEPTUAL QUALITY WIRELESS IMAGE DELIVERY WITH DENOISING DIFFUSION MODELS

Selim F. Yilmaz^{*}, Xueyan Niu[†], Bo Bai[†], Wei Han[†], Lei Deng[†] and Deniz Gündüz^{*†}

^{*}Imperial College London, London, UK, {s.yilmaz21,d.gunduz}@imperial.ac.uk

[†]Huawei Technologies Co. Ltd., {niuxueyan3, baibo8, harvey.hanwei, deng.lei}@huawei.com

ABSTRACT

We consider the image transmission problem over a noisy wireless channel via deep learning-based joint source-channel coding (DeepJSCC) along with a denoising diffusion probabilistic model (DDPM) at the receiver. Specifically, we are interested in the perception-distortion trade-off in the practical finite block length regime, in which separate source and channel coding can be highly suboptimal. We introduce a novel scheme that utilizes the range-null space decomposition of the target image. We transmit the range-space of the image after encoding and employ DDPM to progressively refine its null space contents. Through extensive experiments, we demonstrate significant improvements in distortion and perceptual quality of reconstructed images compared to standard DeepJSCC and the state-of-the-art generative learning-based method. We will publicly share our source code to facilitate further research and reproducibility.

Index Terms— Joint source-channel coding, denoising diffusion models, generative learning, wireless image delivery.

1. INTRODUCTION

Traditional wireless communication systems have two components: source coding and channel coding. Source coding compresses signals by removing data redundancies, while channel coding introduces structured redundancy to improve resilience against channel noise. For wireless image transmission, compression codecs like JPEG or BPG are used to reduce communication resources, but this also lowers the reconstructed image quality. To ensure reliable transmission over a noisy channel, channel coding methods like LDPC, turbo codes, or polar coding are applied. Shannon proved the optimality of this separation-based design in the asymptotic infinite blocklength regime [1]. However, optimality of separation does not hold in real-world scenarios with finite blocklengths. Moreover, suboptimality gap between separation-based and joint schemes enlarges as the blocklength

or the channel signal-to-noise ratio (SNR) decreases, and such conditions are becoming increasingly more relevant for time-sensitive Internet of Things (IoT) applications [2].

Alternative joint source-channel coding (JSCC) schemes have long been studied in the literature; however, they have not found applications in practice due to their high complexity and/or limited performance gains with real sources and channels [3–5]. Recently, there is renewed interest in JSCC due to the use of deep neural networks (DNNs), called deep joint source-channel coding (DeepJSCC) [6]. This method models the communication system as a data-driven autoencoder architecture. Follow-up studies on DeepJSCC have shown that it can exploit feedback, improve performance by increasing the filter size, and adapt to varying channel bandwidth and SNR conditions with almost no loss in performance [7–12]. It is important to note that DeepJSCC avoids the *cliff effect* and achieves *graceful degradation*, which means that the image can still be decoded even if the channel quality falls below the target SNR, although with lower reconstruction quality. This provides a major advantage of DeepJSCC compared to separation-based conventional alternatives when accurate channel modelling and estimation is challenging [13, 14]. A diffusion-based hybrid DeepJSCC scheme is also considered in [15].

Standard DeepJSCC for images focused only on the distortion of the reconstructed image with respect to the input. On the other hand, there has been significant progress in recent years in generative models that generate realistic images with better perception qualities. In [11], adversarial loss has been used for DeepJSCC to improve the perceptual quality of the reconstructed images; however this has achieved limited success due to the difficulties in training generative adversarial network (GAN) models. Alternatively, the authors of [16] employed StyleGAN2, a powerful pretrained generative model to improve the perceptual quality of the image reconstructed by DeepJSCC by modeling the whole encoder-channel-decoder pipeline as a forward process, and modelling the image reconstruction as an inverse problem. In this paper, we follow a similar approach, but use a diffusion-based generative model at the decoder. Our method outperforms both standard DeepJSCC and GAN-based DeepJSCC of [16] on both perception-oriented and distortion-oriented metrics.

The present work has received funding from the European Union’s Horizon 2020 Marie Skłodowska Curie Innovative Training Network Greenedge (GA. No. 953775) and from CHIST-ERA project SONATA (CHIST-ERA-20-SICT-004) funded by EPSRC-EP/W035960/1.

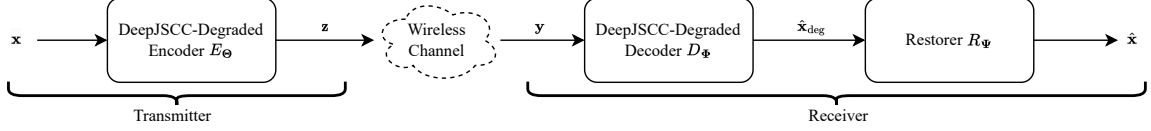


Fig. 1. Overview of the image transmission procedure using our method.

Our main contributions are summarized as follows:

1. We introduce the first denoising diffusion probabilistic model (DDPM)-based DeepJSCC scheme for wireless image delivery that utilizes a novel controlled degradation and restoration-based formulation.
2. Through an extensive set of experiments, we demonstrate that our method outperforms conventional DeepJSCC and previous state-of-the-art generative learning based DeepJSCC for all evaluated SNR and bandwidth conditions.
3. To facilitate further research and reproducibility, we provide the source code of our framework and simulations on github.com/ipc-lab/deepjsc-diffusion.

2. PROBLEM DEFINITION AND METHODOLOGY

Here, we describe the target problem and our novel methodology that combines diffusion models with modified DeepJSCC. We decompose our problem into two stages: (1) autoencoding stage, and (2) restoration stage, which are summarized in Figure 1.

2.1. System Model

We consider wireless image transmission over an additive white Gaussian noise (AWGN) channel with noise variance σ^2 . The transmitter maps an input image $\mathbf{x} \in \mathbb{I}^{C_{in} \times W \times H}$, where W and H denote the width and height of the image, while C_{in} represents the R, G and B channels for colored images, with a non-linear encoding function $E_{\Theta, \sigma} : \mathbb{I}^{C_{in} \times W \times H} \rightarrow \mathbb{C}^k$ parameterized by Θ into a complex-valued latent vector $\tilde{\mathbf{z}} = E_{\Theta}(\mathbf{x}, \sigma)$, where k is the available channel bandwidth. We enforce average transmission power constraint P_{avg} on the transmitted signal $\mathbf{z} \in \mathbb{C}^k$:

$$\frac{1}{k} \|\mathbf{z}\|_2^2 \leq P_{avg}. \quad (1)$$

We satisfy the power constraint by normalizing the signal at the encoder output $\tilde{\mathbf{z}}$ via $\mathbf{z} = \sqrt{k P_{avg} / \|\tilde{\mathbf{z}}\|_2^2} \tilde{\mathbf{z}}$. Then, the transmitter transmits \mathbf{z} over the AWGN channel. The received noisy latent vector is given by $\mathbf{y} \in \mathbb{C}^k$ as $\mathbf{y} = \mathbf{z} + \mathbf{n}$, where $\mathbf{n} \in \mathbb{C}^k$ is independent and identically distributed (i.i.d.) complex Gaussian noise term with variance σ^2 , i.e., $\mathbf{n} \sim \mathcal{CN}(\mathbf{0}, \sigma^2 \mathbf{I}_k)$. We consider σ is known at the transmitters and the receiver.

A non-linear decoding function $D_{\Phi} : \mathbb{C}^k \rightarrow \mathbb{I}^{C'_{in} \times W' \times H'}$ at the receiver, parameterized by Φ , reconstructs a degraded version of the original image using the channel output \mathbf{y} , i.e., $\hat{\mathbf{x}}_{deg} = D_{\Phi}(\mathbf{y}, \sigma)$. Lastly, the restorer R_{ψ} restores the image via $\hat{\mathbf{x}} = R_{\psi}(\hat{\mathbf{x}}_{deg})$. Thus, given channel output \mathbf{y} , the flow of data at the receiver becomes $\mathbf{y} \xrightarrow{D_{\Phi}} \hat{\mathbf{x}}_{deg} \xrightarrow{R_{\psi}} \hat{\mathbf{x}}$. Note that, in general, these two steps can be combined into a single decoding step. However, similarly to [16], we are interested in refining the degraded image reconstructed by the DeepJSCC decoder modeled by D_{Φ} to improve its perceptual quality.

The bandwidth ratio ρ characterizes the available channel resources, which is defined as:

$$\rho = \frac{k}{C_{in} W H} \quad \text{channel symbols/pixel.}$$

We also define the SNR, which characterizes the channel quality, as:

$$\text{SNR} = 10 \log_{10} \left(\frac{P_{avg}}{\sigma^2} \right) \text{ dB}. \quad (2)$$

Given ρ and SNR, the goal in general is to minimize the average distortion between the original image \mathbf{x} at the transmitter and the reconstructed image $\hat{\mathbf{x}}$ at the receiver, i.e.,

$$\arg \min_{\Theta, \Phi, \psi} \mathbb{E}_{r(\mathbf{x}, \hat{\mathbf{x}})} [d(\mathbf{x}, \hat{\mathbf{x}})], \quad (3)$$

where $r(\mathbf{x}, \hat{\mathbf{x}})$ is the joint distribution of original image and the reconstructed image and $d(\mathbf{x}, \hat{\mathbf{x}})$ can be any metric. As mentioned, we employ in our architecture the DeepJSCC as the code block, which maximizes the average peak signal to noise ratio (PSNR), defined as:

$$d_{\text{PSNR}}(\mathbf{x}, \hat{\mathbf{x}}) = 10 \log_{10} \left(\frac{A^2}{\frac{1}{C_{in} H W} \|\mathbf{x} - \hat{\mathbf{x}}\|_2^2} \right) \text{ dB}, \quad (4)$$

where A is the maximum possible input value, e.g., $A = 255$ for images with 8-bit per channel as in our case. However, in practice, it is known that PSNR does not necessarily lead to perceptually better reconstructions. Hence, we will also consider the LPIPS metric [17], which has been shown to better match human perception.

2.2. Transmission of Degraded Image

We will treat the process from the input image to the reconstructed degraded image as a forward process, and

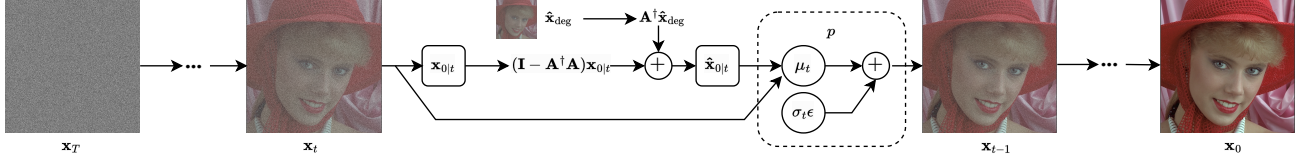


Fig. 2. Overview of the image restoration procedure by R_ψ .

formulate the restorer as an inverse problem. In [16], this was formulated as a stochastic forward process due to the presence of channel noise. Here, we would like to approximate the impact of this forward process as a known linear transform, $\mathbf{A} \in \mathbb{R}^{d \times D^{-1}}$. Hence, the aim of DeepJSCC-Degraded is to transmit a degraded version of \mathbf{x} , denoted by $\mathbf{x}_{\text{deg}} \in \mathbb{R}^{d \times 1}$, where

$$\mathbf{x}_{\text{deg}} = \mathbf{A}\mathbf{x}.$$

Degradation matrix \mathbf{A} can be any linear operator, such as decolorization or mean-pooling-based downsampling [18]. Ideal \mathbf{A} should have the following properties:

1. It should reduce the amount of information to be transmitted so that \mathbf{x}_{deg} can be recovered at the receiver, and the reconstruction error, which follows an unknown distribution, is lower.
2. It should preserve perceptual invariances of the image so that $\hat{\mathbf{x}}_{\text{deg}}$ can be restored by R_ψ yielding a consistent and perceptually high quality image $\hat{\mathbf{x}}$.

When $\mathbf{A} = \mathbf{I}$, our scheme for autoencoding stage is equivalent to the standard DeepJSCC. However, note that, when the channel SNR and bandwidth ratio ρ are low, the receiver cannot recover the desired \mathbf{x}_{deg} , and additional reconstruction error is introduced, following an unknown distribution. Our goal by introducing \mathbf{A} is to obtain a known degradation operator to remove the additional noise and to allow good restoration. For instance, a lower resolution image can be transmitted more reliably on the same channel w.r.t. its higher resolution version, yet, it requires further restoration at the receiver to recover its high resolution version.

2.3. Restoration of Degraded Image

Here, we describe the restoration stage that reverts the known degradation modelled by \mathbf{A} and improves its perceptual quality while remaining as consistent with $\hat{\mathbf{x}}_{\text{deg}}$ as possible.

We denote the pseudo-inverse of \mathbf{A} via \mathbf{A}^\dagger , which satisfies $\mathbf{A}\mathbf{A}^\dagger \mathbf{A} \equiv \mathbf{A}$ and can be solved in matrix form using singular value decomposition (SVD). For instance, \mathbf{A}^\dagger corresponds to upsampling matrix for the downsampling-based degradation

operator \mathbf{A} . Given degraded image \mathbf{x}_{deg} , image restoration (IR) aims to yield $\hat{\mathbf{x}}$ that does not introduce significant distortion while increasing the perceptual quality of the image [18]. For the former, we introduce a consistency constraint that requires $\mathbf{A}\hat{\mathbf{x}} \equiv \mathbf{x}_{\text{deg}}$, whereas the perceptual quality requires $\hat{\mathbf{x}} \sim q(\mathbf{x})$, where $q(\mathbf{x})$ represents the ground-truth (GT) image distribution.

We employ DDPM, denoted by Z_ψ , which is trained through a progressive denoising task. DDPM consists of T-step forward and backward processes. The forward process gradually introduces random noise into the data, whereas the reverse process generates desired data samples from that noise. ϵ denotes the noise in \mathbf{x}_t at timestep t . DDPM utilizes a neural network (NN) Z_ψ to predict the noise ϵ , i.e., $\epsilon_t = Z_\psi(\mathbf{x}_t, t)$ is the estimation of ϵ at time-step t . We refer the reader to [18, 19] for further details on DDPMs due to space constraints. Although DDPMs are powerful unconditional image generators, generating consistent images is challenging [18, 19]. We employ zero-shot image restoration method deep denoising null-space model (DDNM), which utilizes and guides the DDPM model Z_ψ for restoration task to improve quality while preserving consistency. Note that since DDNM utilizes a pretrained DDPM, it does not require specific training for restoration task and improves the applicability of our method [18].

Any sample \mathbf{x} can be decomposed into $\mathbf{x} \equiv \mathbf{A}^\dagger \mathbf{A}\mathbf{x} + (\mathbf{I} - \mathbf{A}^\dagger \mathbf{A})\mathbf{x}$, called range-null space decomposition, where the two terms correspond to range and null space, respectively. We denote the estimated \mathbf{x}_0 at diffusion time-step t as $\mathbf{x}_{0|t}$. For a degraded image \mathbf{x}_{deg} , we can construct a solution for $\hat{\mathbf{x}}$ that satisfies the consistency constraint:

$$\hat{\mathbf{x}} = \mathbf{A}^\dagger \mathbf{x}_{\text{deg}} + (\mathbf{I} - \mathbf{A}^\dagger \mathbf{A})\mathbf{x}_{0|t},$$

where $\mathbf{x}_{0|t}$ is iteratively refined via the procedure shown in Figure 2 and Algorithm 1, where $\bar{\alpha}$ is a hyperparameter determining the noise schedule and p is the forward diffusion process distribution (see [18]). Since modifying $\mathbf{x}_{0|t}$ does not affect the consistency constraint, the restoration procedure does not break consistency of the transmitted image. Therefore, we refine the image to increase its perceptual quality while keeping it consistent to the version reconstructed by the DeepJSCC decoder with a known degradation. Finally, we unflatten $\hat{\mathbf{x}}$ back to the dimensions $C_{\text{in}} \times W \times H$.

¹We consider flattened versions of \mathbf{x} , \mathbf{x}_{deg} , $\hat{\mathbf{x}}$ and $\hat{\mathbf{x}}$ for simplicity of the notation, e.g., we map $\mathbf{x} \in \mathbb{R}^{C_{\text{in}} \times W \times H}$ to $\mathbf{x} \in \mathbb{R}^{D \times 1}$, where $D = C_{\text{in}}WH$.

Algorithm 1 Image restoration procedure R_Ψ .

```

1:  $\mathbf{x}_T \sim \mathcal{N}(\mathbf{0}, \mathbf{I})$   $\triangleright$  Initialize from pure noise
2: for  $t = T, \dots, 1$  do
3:    $\mathbf{x}_{0|t} = \frac{1}{\sqrt{\alpha_t}} (\mathbf{x}_t - Z_\Psi(\mathbf{x}_t, t) \sqrt{1 - \alpha_t})$   $\triangleright$  Denoising step
4:    $\hat{\mathbf{x}}_{0|t} = \mathbf{A}^\dagger \hat{\mathbf{x}}_{\text{deg}} + (\mathbf{I} - \mathbf{A}^\dagger \mathbf{A}) \mathbf{x}_{0|t}$   $\triangleright$  Refine null-space
5:    $\mathbf{x}_{t-1} \sim p(\mathbf{x}_{t-1} | \mathbf{x}_t, \hat{\mathbf{x}}_{0|t})$   $\triangleright$  Sample from reverse process
6: return  $\mathbf{x}_0$ 

```

2.4. Autoencoder Network Architecture and Training

For the autoencoding stage of our method, we first construct deep convolutional neural network (CNN) and autoencoder-based architecture following previous DeepJSCC works [6, 7]. CNNs allow extracting high-level features by exploiting spatial structures within high dimensional inputs such as images, and has been known to perform well for various vision-related tasks [6]. We employ an architecture that is similar to [20] that has nearly symmetric encoder and decoders. It also has residual connections and computationally efficient attention mechanism [21]. We utilize attention feature (AF) module to prevent significant performance degradation for different SNRs [10]. We randomly sample SNR values during training since AF module requires SNR as an input.

Notice that our CNN-based autoencoder reconstructs the degraded image $\hat{\mathbf{x}}_{\text{deg}}$ instead of $\hat{\mathbf{x}}$ unlike the current DeepJSCCs architectures [6, 20]. We instead construct a CNN-based decoder D_Φ that reconstructs $\hat{\mathbf{x}}_{\text{deg}}$, which is later restored by R_Ψ . We denote degradation matrix \mathbf{A} to be the average pooling matrix (with downsampling factor of 2 on both dimensions), so we have $2W' = W$, $2H' = H$ and $C_{\text{in}} = C'_{\text{in}}$. The reason for this choice is because we can reliably revert this degradation and obtain a high quality image via restoration as described in Section 2.3. For fair comparison, we employ the same NN architecture with [16] as our autoencoder, except that we replace the first residual upsample block of the decoder with a residual block to produce the degraded image $\hat{\mathbf{x}}_{\text{deg}}$. For further details on the architecture, please see the Figure 4 of [16].

We first train the encoder and decoder parameters Θ and Φ to minimize the mean squared error (MSE) loss:

$$\mathcal{L}(\mathbf{x}, \hat{\mathbf{x}}_{\text{deg}}) = \frac{1}{C_{\text{in}}WH} \|\mathbf{A}\mathbf{x} - \hat{\mathbf{x}}_{\text{deg}}\|_2^2,$$

which aids our DeepJSCC-Degraded model to transmit degraded instances with minimal distortion with respect to the known degradation modelled by \mathbf{A} .

3. NUMERICAL RESULTS

3.1. Experimental Setup and Implementation Details

We evaluate our method on 512x512 CelebA-HQ dataset, which contains 30 000 high resolution images [22]. We split the dataset using the same procedure as in [16], i.e., split as 8 : 1 : 1 for training, validation, and testing, respectively. We use the PSNR and learned perceptual image patch similarity

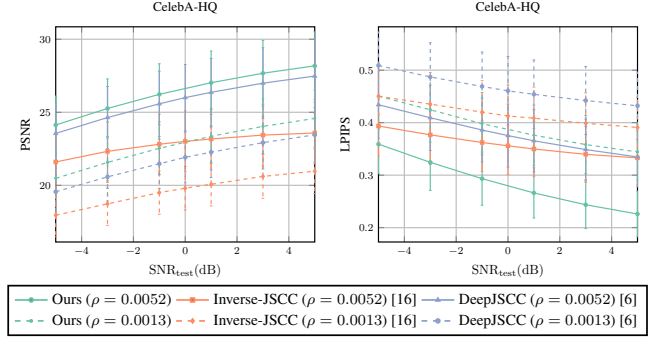


Fig. 3. PSNR and LPIPS comparison of our method with the baselines for $\rho \in \{0.0013, 0.0052\}$ over different SNRs.

(LPIPS) metrics to evaluate the quality of the reconstructed images. LPIPS is a perception metric [17], which computes the similarity between the activations of two image patches for a pre-defined neural network, such as VGG or AlexNet. Note that, a lower LPIPS score is better since it means that image patches are perceptually more similar.

We have conducted the experiments using Pytorch framework [23]. We use the same hyperparameters and the same architecture for all the methods. We set the learning rate as 1×10^{-4} , number of filters in middle layers as 128, batch size as 64 and the power constraint as $P_{\text{avg}} = 1$. We use Adam optimizer [24]. We continue training until no improvement is achieved for consecutive 10 epochs. During training and validation, we run the model using different SNR values for each instance, uniformly chosen from $[-5, 5]$ dB. We test and report the results for each SNR value using the same model thanks to the AF module. We shuffle the training pairs or instances randomly before each epoch.

In the restoration step, we employ 512x512 unconditional Imagenet DDPM, which is fine-tuned for 8100 steps from OpenAI’s class-conditional DDPM [19]. We set the number of diffusion timesteps to $T = 1000$ with linear schedule. We also utilize the time-travel trick in [18] with 100 sampling timesteps.

3.2. Comparison with the Baselines

In this section, we show the superiority of our method over standard DeepJSCC and GAN-based DeepJSCC [16], named Inverse-JSCC. Since previous studies have already shown that DeepJSCC outperforms classical separation-based methods, we do not consider them as baselines [6].

Figure 3 shows the comparisons in terms of PSNR and LPIPS metrics, respectively. We highlight that we consider an extremely challenging communication scenario with a very low bandwidth ratio. Our method clearly improves w.r.t. both DeepJSCC and Inverse-JSCC at all evaluated values of $\text{SNR}_{\text{test}} \in [-5, 5]$ dB and $\rho \in \{0.0013, 0.0052\}$. Figure 4 shows an example set of reconstructed images for qualitative comparison. It is clear that the proposed method generates

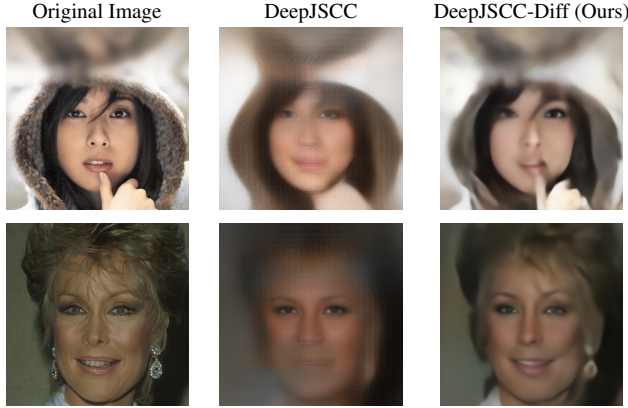


Fig. 4. Qualitative comparison of the reconstructed images from CelebA-HQ dataset for $\rho = 0.0013$ and $\text{SNR}_{\text{test}} = 3$ dB.

more realistic images, but surprisingly, it also achieves a much lower distortion at all channel conditions. We note that our method improves upon DeepJSCC even in terms of the distortion metric, PSNR. This shows that it is beneficial for the DeepJSCC encoder/decoder to target to deliver a lower resolution version of the image, which can then be improved at the receiver using the diffusion model.

4. CONCLUSION

We have introduced a novel generative communication scheme for image transmission over noisy wireless channels, which promotes realness and consistency through controlled degraded image transmission followed by restoration. The introduced method employs DDPM in addition to a modified DeepJSCC, which aims at transmitting a degraded image with the degradation modeled as a known linear transform. We have shown that the proposed scheme outperforms the standard DeepJSCC and the state-of-the-art GAN-based DeepJSCC. While we have considered a specific linear transform for the DeepJSCC encoder/decoder pair in this work, we will consider its optimization in our future work.

5. REFERENCES

- [1] Claude Shannon, “A mathematical theory of communication,” *The Bell System Technical Journal*, vol. 27, no. 3, pp. 379–423, 1948.
- [2] Messaoud Doudou, Djamel Djenouri, and Nadjib Badache, “Survey on latency issues of asynchronous MAC protocols in delay-sensitive wireless sensor networks,” *IEEE Communications Surveys & Tutorials*, vol. 15, no. 2, pp. 528–550, 2012.
- [3] Kannan Ramchandran, Antonio Ortega, K. Metin Uz, and Martin Vetterli, “Multiresolution broadcast for digital hdtv using joint source/channel coding,” *IEEE Journal on Selected Areas in Communications*, vol. 11, no. 1, pp. 6–23, 1993.
- [4] Fan Zhai, Yiftach Eisenberg, and Aggelos K Katsaggelos, “Joint source-channel coding for video communications,” *Handbook of Image and Video Processing*, pp. 1065–1082, 2005.
- [5] Ozgun Y Bursalioglu, Giuseppe Caire, and Dariush Divsalar, “Joint source-channel coding for deep-space image transmission using rateless codes,” *IEEE Transactions on Communications*, vol. 61, no. 8, pp. 3448–3461, 2013.
- [6] Eirina Bourtsoulatzé, David Burth Kurka, and Deniz Gündüz, “Deep joint source-channel coding for wireless image transmission,” *IEEE Transactions on Cognitive Communications and Networking*, vol. 5, no. 3, pp. 567–579, 2019.
- [7] David Burth Kurka and Deniz Gündüz, “Deepjsc-f: Deep joint source-channel coding of images with feedback,” *IEEE Journal on Selected Areas in Information Theory*, vol. 1, no. 1, pp. 178–193, 2020.
- [8] David Burth Kurka and Deniz Gündüz, “Joint source-channel coding of images with (not very) deep learning,” in *International Zurich Seminar on Information and Communication (IZS 2020). Proceedings*. ETH Zurich, 2020, pp. 90–94.
- [9] David Burth Kurka and Deniz Gündüz, “Bandwidth-agile image transmission with deep joint source-channel coding,” *IEEE Transactions on Wireless Communications*, vol. 20, no. 12, pp. 8081–8095, 2021.
- [10] Jialong Xu, Bo Ai, Wei Chen, Ang Yang, Peng Sun, and Miguel Rodrigues, “Wireless image transmission using deep source channel coding with attention modules,” *IEEE Transactions on Circuits and Systems for Video Technology*, vol. 32, no. 4, pp. 2315–2328, 2021.
- [11] Mingyu Yang, Chenghong Bian, and Hun-Seok Kim, “OFDM-guided deep joint source channel coding for wireless multipath fading channels,” *IEEE Transactions on Cognitive Communications and Networking*, vol. 8, no. 2, pp. 584–599, 2022.
- [12] Haotian Wu, Yulin Shao, Krystian Mikolajczyk, and Deniz Gündüz, “Channel-adaptive wireless image transmission with ofdm,” *IEEE Wireless Communications Letters*, vol. 11, no. 11, pp. 2400–2404, 2022.
- [13] Khizar Anjum, Zhuoran Qi, and Dario Pompili, “Deep joint source-channel coding for underwater image

- transmission,” in *Proc. International Conf. on Underwater Nets. & Systems*, New York, NY, USA, 2022.
- [14] Haotian Wu, Yulin Shao, Chenghong Bian, Krystian Mikolajczyk, and Deniz Gündüz, “Deep joint source-channel coding for adaptive image transmission over MIMO channels,” *arXiv:2309.00470*, 2023.
 - [15] Xueyan Niu, Xu Wang, Deniz Gündüz, Bo Bai, Weichao Chen, and Guohua Zhou, “A hybrid wireless image transmission scheme with diffusion,” in *Proc. of IEEE Int’l Workshop on Signal Proc. Adv. in Wireless Comm. (SPAWC)*, 2023.
 - [16] Ecenaz Erdemir, Tze-Yang Tung, Pier Luigi Dragotti, and Deniz Gündüz, “Generative joint source-channel coding for semantic image transmission,” *IEEE Journal on Selected Areas in Communications*, vol. 41, no. 8, pp. 2645–2657, 2023.
 - [17] Richard Zhang, Phillip Isola, Alexei A Efros, Eli Shechtman, and Oliver Wang, “The unreasonable effectiveness of deep features as a perceptual metric,” in *Proceedings of the IEEE conference on computer vision and pattern recognition*, 2018, pp. 586–595.
 - [18] Yinhuai Wang, Jiwen Yu, and Jian Zhang, “Zero-shot image restoration using denoising diffusion null-space model,” *The Eleventh International Conference on Learning Representations*, 2023.
 - [19] Prafulla Dhariwal and Alexander Nichol, “Diffusion models beat gans on image synthesis,” *Advances in neural information processing systems*, vol. 34, pp. 8780–8794, 2021.
 - [20] Tze-Yang Tung, David Burth Kurka, Mikolaj Jankowski, and Deniz Gündüz, “Deepjscc-q: Channel input constrained deep joint source-channel coding,” in *IEEE International Conference on Communications*, 2022, pp. 3880–3885.
 - [21] Zhengxue Cheng, Heming Sun, Masaru Takeuchi, and Jiro Katto, “Learned image compression with discretized Gaussian mixture likelihoods and attention modules,” in *Proceedings of the IEEE/CVF Conference on Computer Vision and Pattern Recognition*, 2020, pp. 7939–7948.
 - [22] Tero Karras, Timo Aila, Samuli Laine, and Jaakko Lehtinen, “Progressive growing of GANs for improved quality, stability, and variation,” in *International Conference on Learning Representations*, 2018.
 - [23] Adam Paszke, Sam Gross, Francisco Massa, Adam Lerer, James Bradbury, Gregory Chanan, Trevor Killeen, Zeming Lin, Natalia Gimelshein, Luca Antiga, et al., “Pytorch: An imperative style, high-performance deep learning library,” *Advances in Neural Information Processing Systems*, vol. 32, 2019.
 - [24] Diederik P Kingma and Jimmy Ba, “Adam: A method for stochastic optimization,” *arXiv preprint arXiv:1412.6980*, 2014.